EurJIC
European Journal of Inorganic Chemistry

A Journal of ChemPubSoc Europe

Accepted Article

Title: Synthesis of a T-Shaped Cobalt(I) Complex and its Dinitrogen Adduct

Authors: Corey Sanz, Carolin Stein, and Michael D. Fryzuk

To be cited as: *Eur. J. Inorg. Chem.* 10.1002/ejic.201901129

Link to VoR: http://dx.doi.org/10.1002/ejic.201901129

WILEY-VCH

10.1002/ejic.201901129

WILEY-VCH

Synthesis of a T-Shaped Cobalt(I) Complex and its Dinitrogen Adduct

Corey A. Sanz,[a] Carolin A. M. Stein,[a] and Michael D. Fryzuk*[a]

Abstract: The coordination chemistry of the new NNP pincer ligand framework (QuiNacNacP) is explored with cobalt. Upon treatment of the cobalt(II) complex **Co[QuiNacNacP]Cl** with KC_8, the formation of cobalt(I) dinitrogen complex **Co[QuiNacNacP]N_2** was observed. **Co[QuiNacNacP]N_2** crystallizes as a square planar (S = 0) complex with an essentially unactivated N_2 ligand. In solution, the dinitrogen complex is in equilibrium with the paramagnetic T-shaped complex **Co[QuiNacNacP]** (S = 1). The ability of **Co[QuiNacNacP]Cl** to act as a catalyst precursor in the reductive silylation of dinitrogen was also briefly explored. Reaction of ~1000 equivalents KC_8 with ~1500 equivalents Me_3SiCl (relative to **Co[QuiNacNacP]Cl**) under 1 atm of N_2 furnished roughly 40 equivalents of $N(SiMe_3)_3$.

Introduction

Activation of small neutral molecules by soluble metal complexes requires interaction with the metal usually via an open site in the coordination sphere. While many strategies exist for particular geometries, recently T-shaped metal ligand environments have been shown to be effective as catalyst precursors for a number of processes involving small molecules.[1] Pincer ligands are of course the most famous for their ability to generate T-shaped environments, but other tridentate donor sets are known.[2]

One of the advantages of ligand sets that can support T-shaped environments is that addition of a fourth ligand can allow formation of square planar or tetrahedral structures, sometimes with minimal change in the ligand structure but with considerable change in the electronic structure of the metal center. For example, T-shaped d^8 metal complexes are S = 1 systems that change to S = 0 by addition of ligands that generate square-planar complexes, whereas formation of d^8 tetrahedral complexes remain S = 1.

We recently reported[3] the T-shaped cobalt complex **Co[NpNP]** (Figure 1) that is remarkably efficient in the catalytic silylation of dinitrogen under reducing conditions.[4,5] We have been interested in using this ligand framework as a starting point to explore other related ligand designs and their metal complexes in catalysis. In this work, we present a tridentate ligand set that can support T-shaped environments and examine its coordination chemistry with cobalt.

As previously mentioned, **Co[NpNP]** can be isolated as an authentic T-shaped complex that has μ_{eff} = 2.4 μ_B. Under an atmosphere of N_2, it generates the distorted tetrahedral dinitrogen complex **Co[NpNP]N_2**, which is also paramagnetic. In the presence of excess KC_8 and Me_3SiCl, this cobalt system acts as an effective catalyst for the production of $N(SiMe_3)_3$ from N_2 (1 atm) at -40°C, generating ≥ 200 equivalents per mol of catalyst precursor.[3]

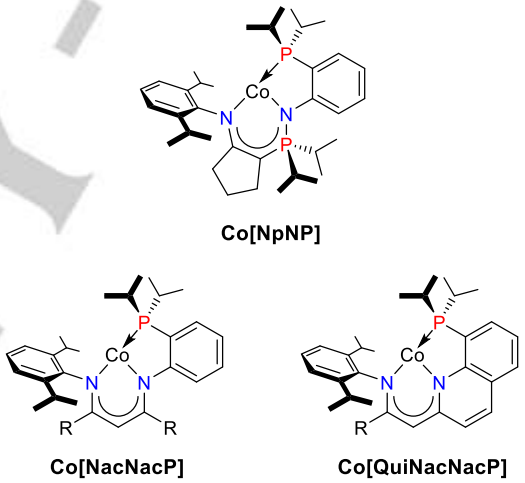

Figure 1. T-shaped cobalt(I) complexes with anionic NNP pincer ligands.

Based on the environment that the NpNP donor set provides in **Co[NpNP]**, we targeted two environments that would replicate the steric and electronic environments found in NpNP, that is, a tridentate NNP donor set with a delocalized negative charge, and identical substituents decorating the imine/enamine and phosphine units. As shown in Figure 1, we are focusing on two targets: **Co[NacNacP]** and **Co[QuiNacNacP]**. In this work we present our studies on the preparation and coordination chemistry of the QuiNacNacP system.

Results and Discussion

Synthesis of Li[QuiNacNacP]

The QuiNacNacP ligand was selected on the basis of several structural features that are shared with phosphinimine

[a] Dr. C. A. Sanz, Ms. C. A. M. Stein, Prof. M. D. Fryzuk
Department of Chemistry
The University of British Columbia
2036 Main Mall
Vancouver, BC, Canada V6T 1Z1
E-mail: Fryzuk@chem.ubc.ca
Homepage: https://www.chem.ubc.ca/michael-fryzuk

Supporting information for this article is given via a link at the end of the document.

ligand NpNP. The NN chelating component of the QuiNacNacP ligand is reminiscent of the well-known family of NacNac ligands.[6] The π system of the NacNac fragment in QuiNacNacP is expanded through the installation of a fused quinoline group.

Scheme 1 outlines the synthesis of **Li[QuiNacNacP]**. Bromo-substituted quinoline **1** is prepared according to a previously reported procedure *via* a Doeber-Miller reaction.[7] The diisopropylphosphine is then installed through a Pd-catalyzed P-C coupling reaction.[8] Reaction of phosphine-substituted quinoline **2** with lithium diisopropylamide (LDA) followed by imidoyl chloride **3** furnishes **Li[QuiNacNacP]** in excellent yield. The second equivalent of LDA used in this reaction is crucial because it prevents neutral (protonated) **H[QuiNacNacP]** from quenching the deprotonated starting material.

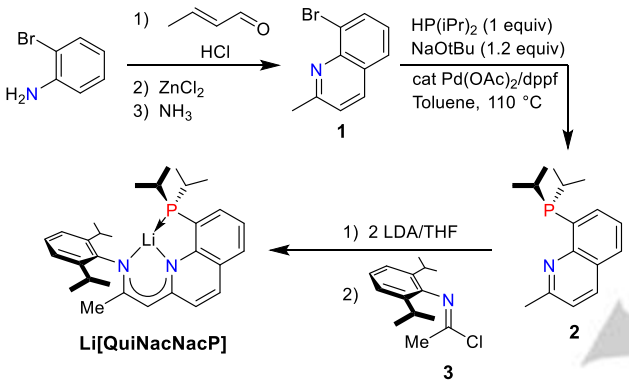

Scheme 1. Synthesis of **Li[QuiNacNacP]**. dppf = 1,1'-bis(diphenylphosphino)-ferrocene; LDA = lithium diisopropylamide.

Synthesis and Characterization of Co[QuiNacNacP]Cl

Treatment of **Li[QuiNacNacP]** with one equivalent of $CoCl_2$ in THF generated the cobalt(II) chloride complex **Co[QuiNacNacP]Cl** (Scheme 2). The ^{1}H NMR spectrum of **Co[QuiNacNacP]Cl** contains broadened signals over a wide range of chemical shifts (+/- 100 ppm) indicative of a paramagnetic complex (see Figure S6 in the SI). The magnetic moment of **Co[QuiNacNacP]Cl** in solution (Evans method) is 3.75 μ_B, which is consistent with a tetrahedral d^7 metal center with 3 unpaired electrons (S = 3/2).

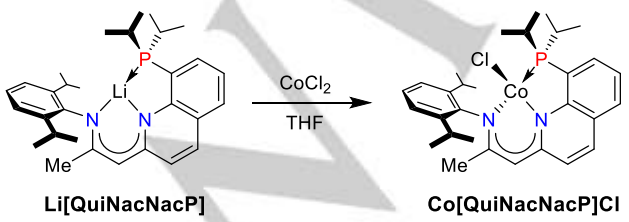

Scheme 2. Synthesis of cobalt chloride complex **Co[QuiNacNacP]Cl**.

The X-ray structure of **Co[QuiNacNacP]Cl** (Figure 2) displays a pseudo-tetrahedral geometry around the cobalt atom. The large P-Co-N1 angle (136°) can be ascribed to the size constraints enforced by the rigid scaffold of the planar ligand core.

The depiction of highly conjugated molecules using distinct single and double bonds is misleading. Based on the bond lengths discussed below, the delocalized formulation shown in Scheme 2 is reasonably accurate. In particular, the C2-C3 and C3-C4 bond lengths are exactly the same length at 1.396(4) Å, and both C2-N1 and C4-N2 are of similar length at 1.340(3) and 1.354(3) Å, respectively. In fact, the C2-C3/C3-C4 bond lengths are in very good agreement with those of other NacNac Co(II) complexes.[9] The C2-N1 bond length (1.340(3) Å) is also very similar to those observed in other NacNac ligands, while the C4-N2 bond (1.354(3) Å) is slightly longer.[9] The C4-N2 bond, however, is much longer than the analogous CN bond of other quinoline ligands bound to Co(II) (~1.31 Å).[10] This suggests the delocalized depiction of **Co[QuiNacNacP]Cl** shown in Scheme 2 is appropriate.

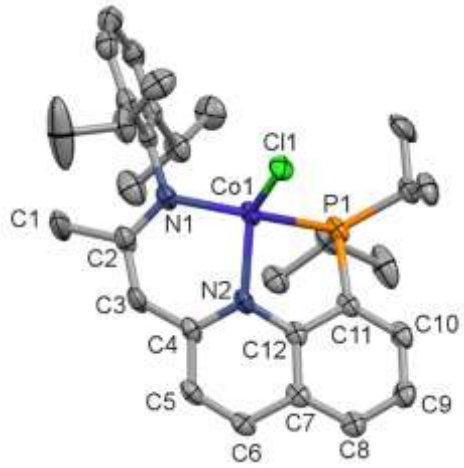

Figure 2. X-ray structure of cobalt(II) chloride complex **Co[QuiNacNacP]Cl**. Hydrogen atoms have been omitted for clarity. Thermal ellipsoids are shown at the 50% probability level.

Reduction of Co[QuiNacNacP]Cl

Cobalt(II) chloride complex **Co[QuiNacNacP]Cl** was reacted with one equivalent of KC_8 and the reaction was monitored by ^{1}H NMR spectroscopy. Over the course of the reaction, the signals belonging to **Co[QuiNacNacP]Cl** disappeared and a new set of paramagnetically shifted peaks appeared (Figure 3). Single crystals of the product were isolated from a saturated diethyl ether solution that was gradually cooled in the freezer overnight. An X-ray diffraction experiment on the brown crystals revealed the formation of dinitrogen complex **Co[QuiNacNacP]N$_2$** (Figure 4; Scheme 3).

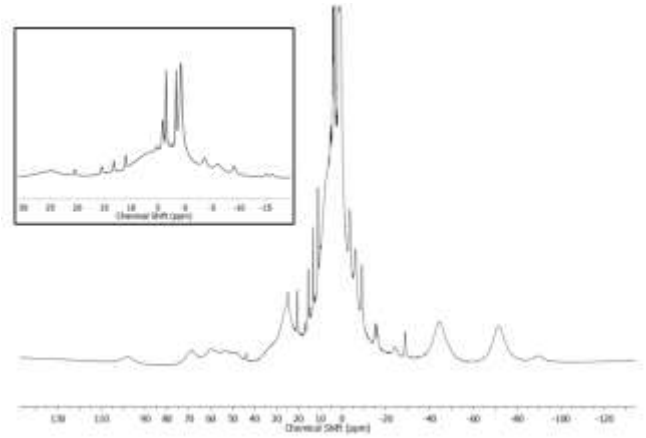

Figure 3. ^{1}H NMR spectrum of the cobalt(I) complex formed *via* the reduction of **Co[QuiNacNacP]Cl** with KC_8 (THF-d_8, 298 K, 1 atm N_2). The inset is an expansion of the spectrum between -20 and +30 ppm.

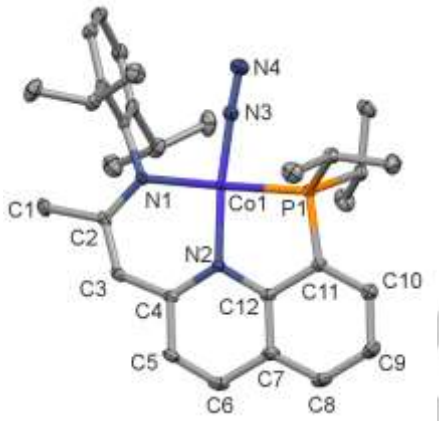

Figure 4. X-ray structure of cobalt(I) dinitrogen complex **Co[QuiNacNacP]N$_2$**. Hydrogen atoms have been omitted for clarity. Thermal ellipsoids are shown at the 50% probability level.

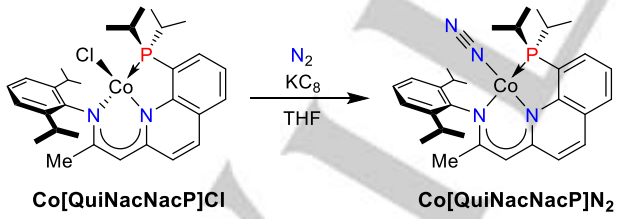

Scheme 3. Reduction of cobalt chloride complex **Co[QuiNacNacP]Cl** under N_2.

The X-ray structure of **Co[QuiNacNacP]N$_2$** (Figure 4) contains an end-on bound dinitrogen ligand coordinated to a square-planar cobalt(I) center (sum of angles = 360°). The N3-N4 bond length of the terminal dinitrogen ligand (1.125(2) Å) is similar to those of other Co(I) complexes with pincer ligands and indicates an essentially unactivated N_2 ligand.[11] The relatively high IR stretching frequency (2042 cm^{-1} in the solid state) supports this claim. The CC bonds in the C1-4 chain and the C2-N1 bond are essentially the same length as those found in cobalt(II) complex **Co[QuiNacNacP]Cl** (Table 1). However, the bonds in the quinoline group, notably the C4-N2 bond, have lengthened following reduction (see Table S1 in the SI). The bonds between cobalt and the heteroatoms of the tridentate pincer ligand are much shorter in **Co[QuiNacNacP]N$_2$** compared to those of **Co[QuiNacNacP]Cl** (Table 1); which is expected on going from tetrahedral Co(II) to square planar Co(I).

Table 1. Selected bond lengths (Å) for cobalt complexes

	Co[QuiNacNacP]Cl	Co[QuiNacNacP]N$_2$
N3-N4	---	1.125(2)
Co-N3	---	1.749(1)
Co-Cl	2.2304(8)	---
Co-N1	1.944(2)	1.929(2)
Co-N2	1.982(2)	1.936(1)
Co-P	2.3753(8)	2.148(1)
C2-N1	1.340(3)	1.333(2)
C1-C2	1.514(4)	1.515(3)
C2-C3	1.396(4)	1.391(2)
C3-C4	1.396(4)	1.394(3)
C4-N2	1.354(3)	1.372(2)

The observation that the cobalt(I) dinitrogen complex **Co[QuiNacNac]N$_2$** is apparently paramagnetic in solution is at odds with the observed square-planar structure in the solid state, which should engender a diamagnetic ground state. We turned to variable temperature NMR spectroscopy as a means to probe the behavior of the cobalt(I) complex in solution. Cooling a THF-d_8 solution of the cobalt(I) complex under 1 atm of N_2 below room temperature revealed the appearance of a new set of signals in the diamagnetic region of the ^{1}H NMR spectrum (Figure 5). A resonance at 75.3 ppm in the ^{31}P{^{1}H} NMR spectrum also began to grow in at temperatures below 258 K (see Figure S1 in the SI). These features are consistent with the square planar complex **Co[QuiNacNacP]N$_2$** existing at lower temperatures in solution. The paramagnetic complex that dominates the spectrum at higher temperatures is likely the T-shaped complex **Co[QuiNacNacP]**, which is in equilibrium with diamagnetic **Co[QuiNacNacP]N$_2$** (Scheme 4). A spectrum of the cobalt(I) complex collected under 1 atm of argon showed

broadened signals at chemical shift ranges expected for a paramagnetic compound (see Figure S3 in the SI). Signals consistent with this paramagnetic compound persisted as the temperature was lowered to 198 K and no diamagnetic signals were observed, further confirming the presence of T-shaped **Co[QuiNacNacP]** under an argon atmosphere. Magnetic moment measurements on the cobalt(I) complex under an argon atmosphere (μ_{eff} = 2.75 μ_B, Evans method at 298 K) are consistent with a T-shaped complex in its triplet spin state (S = 1). Three-coordinate T-shaped geometry is rarely observed with cobalt. To the best of our knowledge, there are only three other examples of authentic T-shaped Co(I) complexes that have been characterized.[3, 12] These complexes were also established as high-spin (S = 1) with similar magnetic moments to that of **Co[QuiNacNacP]**.

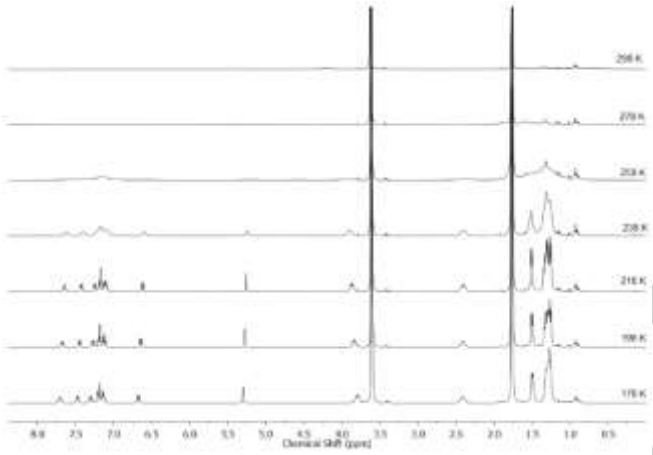

Figure 5. Variable temperature ^{1}H NMR spectra of the cobalt(I) complex formed *via* the reduction of **Co[QuiNacNacP]Cl** with KC_8 (THF-d_8, 1 atm N_2). The singlets at 1.7 and 3.6 ppm are the residual signals from the deuterated solvent.

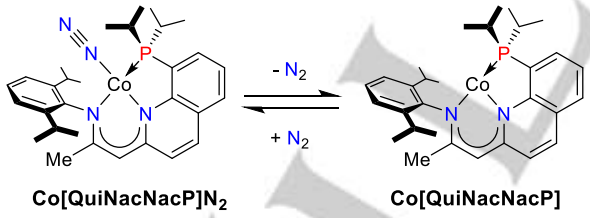

Co[QuiNacNacP]N$_2$ **Co[QuiNacNacP]**

Scheme 4. Equilibrium between square planar **Co[QuiNacNacP]N$_2$** and T-shaped **Co[QuiNacNacP]**.

The equilibrium between **Co[QuiNacNacP]** and **Co[QuiNacNacP]N$_2$** was further explored by measuring the magnetic moment in solution at various temperatures (Evans method, Figure 6). Under 1 atm of nitrogen at room temperature (298 K), the magnetic moment (μ_{eff} = 2.13 μ_B) suggests that paramagnetic **Co[QuiNacNacP]** (S = 1) is the predominant complex in solution. Cooling this solution down results in a decrease in the magnetic moment, consistent with the formation of diamagnetic **Co[QuiNacNacP]N$_2$** at lower temperatures. At 198 K some paramagnetic character still remains (μ_{eff} = 0.79 μ_B). This suggests that some of the T-shaped complex is still present at this temperature.

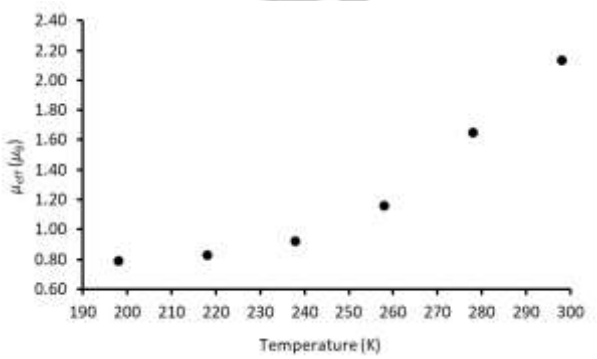

Figure 6. Variable temperature magnetic moment plot for the cobalt(I) complex formed *via* the reduction of **Co[QuiNacNacP]Cl** with KC_8 (Evans method, toluene-d_8)

The magnetic moment of the cobalt(I) complex at 298 K under a nitrogen atmosphere (μ_{eff} = 2.13 μ_B) is lower than that of the T-shaped complex (μ_{eff} = 2.75 μ_B under 1 atm of argon). This suggests that there is still some degree of N_2 binding at room temperature in solution in order to induce spin-pairing and lower the magnetic moment. This hypothesis is supported by IR measurements performed in solution at room temperature. A weak NN stretch was observed at 2051 cm^{-1} in toluene solution, which is slightly higher than the solid-state NN stretching frequency (2042 cm^{-1}). We were unable to observe any signals belonging to **Co[QuiNacNacP]N$_2$** in the ^{1}H NMR spectrum of the cobalt(I) complex at room temperature under 1 atm of nitrogen. However, pressurizing an NMR tube with 4 atm of N_2 revealed a broad signal in the ^{31}P{^{1}H} NMR spectrum (δ = 75 ppm) consistent with dinitrogen complex **Co[QuiNacNacP]N$_2$** (see Figure S4 in the SI).

Catalytic Silylation of Dinitrogen

Phosphinimine complex **Co[NpNP]** was an effective catalyst in the N_2 silylation reaction shown in Scheme 5, despite the low degree of activation found in the dinitrogen ligand.[3] We explored the capability of **Co[QuiNacNacP]Cl** to act as a catalyst precursor in this reaction and the unoptimized catalytic results are presented herein. Treatment of **Co[QuiNacNacP]Cl** with ~1000 equivalents of KC_8 and ~1500 equivalents of Me_3SiCl under 1 atm of N_2 at room temperature yielded 38 turnovers of $N(SiMe_3)_3$. The $N(SiMe_3)_3$ was detected by ^{1}H NMR spectroscopy (see Figure S5 in the SI) and then hydrolyzed to NH_4Cl using HCl. The amount of NH_4Cl produced was quantified using ^{1}H NMR spectroscopy.

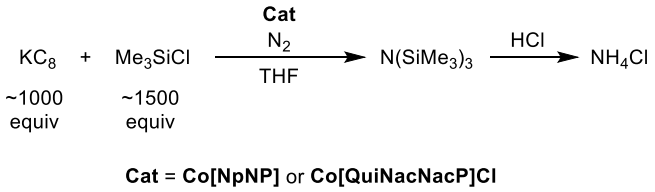

Scheme 5. Catalytic silylation of N_2 to $N(SiMe_3)_3$. The number of equivalents is stated with respect to the cobalt catalyst.

Conclusions

In this work we have reported our first efforts at developing a new ligand system that replicates the environment generated by the enamido-phosphinimine NpNP donor set reported earlier.[3] Because the **Co[NpNP]Cl** and **Co[NpNP]N₂** complexes serve as very efficient catalyst precursors for the silylation of molecular nitrogen, we prepared the quinoline analog, QuiNacNacP, and investigated its coordination chemistry with Co(II) and subsequent reduction to Co(I). Interestingly, the Co(I) complex exists as the square-planar N_2 complex **Co[QuiNacNacP]N₂** in the solid state, but in solution, variable temperature NMR studies are consistent with an equilibrium between the paramagnetic T-shaped **Co[QuiNacNacP]** and the diamagnetic **Co[QuiNacNacP]N₂**. We have also found that this system acts as a catalyst for the formation of $N(SiMe_3)_3$ (38 equiv) using excess KC_8 and Me_3SiCl, albeit under unoptimized conditions. Future work will focus on the effects of different substituents and changes on the backbone of this modular ligand framework, especially as related to catalytic silylation of molecular nitrogen.

Experimental Section

General Considerations: All reactions were carried out under an atmosphere of dinitrogen using standard Schlenk and glovebox techniques. Anhydrous/degassed THF, toluene, diethyl ether, and hexanes were purchased from Sigma and dried further by passing through a column of activated alumina on an Innovative Technology solvent purification system. All deuterated solvents were dried over freshly activated 4 Å molecular sieves and degassed with three freeze-pump-thaw cycles. NMR spectra were recorded on Bruker AV-400 instruments and all chemical shifts and coupling constants are reported in ppm and in Hz, respectively. Solution magnetic moments were determined using Evans method.[13] High resolution mass spectrometry was collected on a JEOL AccutTOF-GC instrument using the EI ionization method in positive mode. Solid state IR data was collected on a Perkin Elmer FT-IR Frontier spectrometer equipped with a Universal ATR sampling accessory. Solution state IR data was collected on a Mettler Toledo ReactIR spectrometer through a capillary fed into a nitrogen filled glovebox. Microanalyses (C, H, N) were performed by the Department of Chemistry at the University of British Columbia. Bromo-substituted quinoline **1**,[7] $HP(^iPr)_2$,[14] imidoyl chloride **3**,[15] and KC_8,[16] were prepared according to literature procedures. All other chemicals were purchased from commercial sources and used without further purification.

8-(diisopropylphosphino)-2-methylquinoline (2): 8.22 g (37 mmol) of **1** was added to a sealable Schlenk bomb equipped with a Teflon plug valve. To the flask was also added 4.28 g (45 mmol) NaO^tBu, 0.82 g (1.5 mmol) dppf (1,1'-Bis(diphenylphosphino)ferrocene), 0.25 g (1.1 mmol) $Pd(OAc)_2$, 8.2 mL $HP(iPr)_2$, and 60 mL of toluene. The flask was sealed and heated to 110 °C for 16 hours. The brownish-purple solution was allowed to cool to room temperature and then the solvent was removed under reduced pressure. The residue was redissolved in 30 mL of diethyl ether and filtered through a short silica plug. The silica was rinsed with a further 30 mL of diethyl ether to afford a brownish-purple solution. The ether was removed under vacuum and the crude product was redissolved in 25 mL of hexanes. After sitting in the freezer overnight, the hexanes solution deposited pale brown-purple crystals. The crystals were isolated by filtration and a further two crops of crystals were obtained from the filtrate by treating it in the same manner as the first crop. The product was isolated as a whitish-purple solid. Yield: 7.513 g (29 mmol, 78%). ^{1}H NMR (C_6D_6, 400 MHz): δ 7.87 (t of d, 1H, $^3J_{HH}$/$^3J_{HP}$ = 7 Hz, ^4J = 1.5 Hz), 7.51 (d, 1H, ^3J = 8 Hz), 7.42 (d of d, 1H, ^3J = 8 Hz, ^4J = 1.5 Hz), 7.20 (t, 1H, ^3J = 8 Hz), 6.75 (d, 1H, ^3J = 8 Hz), 2.74 (sept of d, 2H, $^3J_{HH}$ = 7 Hz, $^2J_{HP}$ = 3 Hz), 2.50 (s, 3H), 1.30 (d of d, 6H, $^3J_{HP}$ = 14 Hz, $^3J_{HH}$ = 7 Hz), 1.01 (d of d, 6H, $^3J_{HP}$ = 12 Hz, $^3J_{HH}$ = 7 Hz). ^{13}C{^{1}H} NMR (C_6D_6, 101 MHz): δ 158.0 (s), 151.3 (d, *J* = 8 Hz), 138.1 (d, *J* = 26 Hz), 136.9 (s), 136.8 (s), 129.1 (s), 127.1 (d, *J* = 1.5 Hz), 125.5 (d, *J* = 7 Hz), 122.0 (s), 25.6 (s), 24.5 (d, *J* = 14 Hz), 21.5 (d, *J* = 20 Hz), 21.1 (d, *J* = 13 Hz). ^{31}P{^{1}H} NMR (C_6D_6, 162 MHz): δ 10.7. HRMS (EI): *m/z* 259.14879 (M^+, Anal. Calcd for $C_{16}H_{22}NP^+$: *m/z* 259.14899). Anal. Calcd for $C_{16}H_{22}NP$: C, 74.10; H, 8.55; N, 5.40. Found: C, 74.05; H, 8.47; N, 5.42

Li[QuiNacNacP]: Lithium diisopropylamide (LDA) was prepared by adding 15.4 mmol of n-butyllithium (9.6 mL of a 1.6 M solution in hexanes) to a solution of diisopropylamine (2.2 mL, 15.6 mmol) in 15 mL of dry THF at -78 °C. The addition was performed in a dry ice / acetone cooling bath and the colorless solution was stirred for five minutes at -78 °C. The cooling bath was then removed and the LDA solution was allowed to stir for 30 minutes at room temperature. A separate solution of **2** (2.00 g, 7.7 mmol) was prepared in 20 mL of THF and cooled to -78 °C. The LDA solution was slowly added to the cooled solution of **2** via syringe. The resulting deep red solution was allowed to stir at -78 °C for 5 minutes before removing the cooling bath. The reaction mixture was then stirred for 1 hour at room temperature. The red solution was cooled back down to -78 °C and then a solution of **3** (1.83 g, 7.7 mmol) in 10 mL of THF was added dropwise. The reaction was stirred for 10 minutes at -78 °C and then 2 hours at room temperature. The solution remained a dark red color throughout the course of the reaction. The solvent was removed under reduced pressure and the resulting red solid was taken back up in 30 mL of toluene. The toluene solution was filtered through a bed of Celite to remove lithium chloride and the filter agent was rinsed with a further 30 mL of toluene. The toluene solution was concentrated to a minimal volume and then hexanes was added to the flask. An orange solid deposited after sitting the freezer overnight. The solid was collected by filtration and a second crop of crystals was obtained by reducing the volume of the filtrate and adding more hexanes. Yield: 2.746 g (5.9 mmol, 76%). ^{1}H NMR (C_6D_6, 400 MHz): δ 7.05-7.20 (m, 6H), 6.84 (t, 1H, *J* = 7 Hz), 6.75 (d, 1H, *J* = 9 Hz), 5.21 (s, 1H), 3.33 (sept, 2H, ^3J = 7 Hz), 1.85 (s, 3H), 1.74 (sept of d, 2H, $^3J_{HH}$ = 7 Hz, $^2J_{HP}$ = 1 Hz), 1.23 (d, 6H, $^3J_{HH}$ = 7 Hz), 1.16 (d, 6H, $^3J_{HH}$ = 7 Hz), 0.66-0.77 (two overlapping d of d, 12H, $^3J_{HH}$ = 7 Hz, $^3J_{HP}$ = 6/7 Hz). ^{13}C{^{1}H} NMR (C_6D_6, 101 MHz): δ 164.3 (s), 157.8 (d, *J* = 2 Hz), 155.6 (d, *J* = 19 Hz), 148.9 (s), 141.1 (s), 133.4 (d, *J* = 4 Hz), 133.1 (d, *J* = 2 Hz), 129.8 (s), 126.7 (s), 124.5 (d, *J* = 5 Hz), 123.9 (s), 123.7 (d, *J* = 6 Hz), 123.5 (s), 119.7 (d, *J* = 2 Hz), 95.2 (s), 28.3 (s), 25.5 (d, *J* = 1 Hz), 23.7 (s), 23.3 (d, *J* = 2 Hz), 23.0 (s), 20.0 (d, *J* = 15 Hz), 18.7 (d, *J* = 6 Hz). ^{31}P{^{1}H} NMR (C_6D_6, 162 MHz): δ -7.6, overlapping 1:1:1:1 quartet ($^2J_{P^7Li}$ = 60 Hz) and 1:1:1 triplet ($^2J_{P^6Li}$ = 22 Hz). HRMS (EI): *m/z* 460.30129 ([M+H], Anal. Calcd for $C_{30}H_{41}N_2P$: *m/z* 460.30073). Anal. Calcd for $C_{30}H_{40}N_2PLi$: C, 77.23; H, 8.64; N, 6.00. Found: C, 76.94; H, 8.83; N, 5.83.

Co[QuiNacNacP]Cl: 0.278 g (2.1 mmol) $CoCl_2$ was suspended in 20 mL of THF. To the suspension was added a solution of **Li[QuiNacNacP]** (1.00 g, 2.1 mmol) in 20 mL of THF. The colour of the solution changed to brown over a period of 16 hours. The solvent was removed under reduced pressure and the residue was redissolved in 30 mL of toluene. The brown solution was filtered through Celite and the filter agent was rinsed with more toluene. The solution was then concentrated and hexanes was added. Brown crystals deposited after sitting overnight at -30 °C. Yield: 0.730 g (1.3 mmol, 63%). Crystals suitable for X-ray diffraction were grown from slow vapour diffusion of hexanes into a concentrated toluene solution. ^{1}H NMR (THF-d_8, 400 MHz): δ 82.55, 36.79, 27.27, 24.50, 22.67, 20.45, 10.35, -2.28, -6.97, -9.36, -10.72, -12.34, -96.66. μ_{eff} = 3.75 μ_B (Evans Method, THF-d_8). HRMS (EI): *m/z* 553.19378 (M^+, Anal. Calcd for $C_{30}H_{40}N_2PCoCl^+$: *m/z* 553.19496). Anal. Calcd for $C_{30}H_{40}N_2PCoCl$: C, 65.04; H, 7.28; N, 5.06. Found: C, 65.07; H, 7.26; N, 5.06. CCDC 1959514.

Co[QuiNacNacP]N_2: 0.356 g (0.64 mmol) **Co[QuiNacNacP]Cl** was added to a Schlenk flask along with 0.091 g (0.67 mmol) KC_8. 10 mL of THF was added to the flask via syringe and the brown solution was stirred under 1 atm of dynamic N_2 overnight. After 18 hours of stirring, the reaction mixture was still dark brown, however, the gold hue of the KC_8 had faded to black. The solvent was removed *in vacuo* and the crude product was taken up in 20 mL of diethyl ether. The ether solution was filtered through a bed of Celite and the filter agent was rinsed with a further 10 mL of diethyl ether. The filtrate was concentrated to a volume of about 5 mL and was then allowed to crystallize in the freezer overnight. The brown crystals were isolated by filtration and rinsed with hexanes. Yield: 0.211 g (0.39 mmol, 60%). Large block crystals suitable for X-ray diffraction were grown from slow cooling of a saturated diethyl ether solution. ^{1}H NMR (THF-d_8, 400 MHz, 178 K): δ 7.68 (t, 1H, *J* = 7 Hz), 7.45 (d, 1H, *J* = 7 Hz), 7.27 (d, 1H, *J* = 9 Hz), 7.45 (d, 1H, *J* = 7 Hz), 7.05-7.20 (m, 4H), 6.65 (d, 1H, *J* = 9 Hz), 5.27 (s, 1H), 3.77 (broad sept, 2H, *J* = 7 Hz), 2.30-2.45 (m, 2H), 1.48 (d, 6H, *J* = 6 Hz), 1.20-1.35 (m, 18H). ^{31}P{^{1}H} NMR (THF-d_8, 162 MHz, 178 K): δ 75.3. IR: 2042 cm^{-1} (crystalline solid, ATR), 2051 cm^{-1} (toluene solution). HRMS (EI): *m/z* 518.22456 ([Co(QuiNacNacP)]$^+$, Anal. Calcd for $C_{30}H_{40}N_2PCo^+$: *m/z* 518.22611). Elemental analysis shows a low value for N due to the labile N_2 ligand. Anal. Calcd for $C_{30}H_{40}N_4PCo$: C, 65.92; H, 7.38; N, 10.25. Found: C, 66.10; H, 7.49; N, 8.78. CCDC 1959515.

Typical procedure for the catalytic silylation of N_2 to $N(SiMe_3)_3$ and hydrolysis to form NH_4Cl: In a glovebox, 0.038 g (0.069 mmol) of **Co[QuiNacNacP]Cl** was added to a 10 mL volumetric flask and the flask was filled to the mark with THF. This stock catalyst solution was transferred to a Schlenk flask and taken out of the glovebox. Separately, a Schlenk flask was charged with 0.956 g (7.07 mmol) KC_8 and 10 mL THF. To this KC_8 suspension was added 1.0 mL of the stock catalyst solution and 1.3 mL of Me_3SiCl by syringe. The brown solution was allowed to stir overnight. Over a period of 17 hours, the brown solution with gold KC_8 flakes changed to a pale yellow solution with black graphite flakes. The graphite and KCl were removed by cannula filtration to afford a clear pale yellow solution. 5 mL of a 1.0 M HCl solution in diethyl ether was added to the flask to form a cloudy yellow solution. The volatiles were then removed under reduced pressure to reveal an oil. The amount of NH_4Cl was determined by NMR spectroscopy in DMSO-d_6 using 1,3,5-trimethoxybenzene as an internal standard according to the procedure reported by Mock and co-workers.[4n]

Acknowledgments

MDF thanks NSERC of Canada for a Discovery grant.

Keywords: dinitrogen • cobalt • catalytic silylation • tridentate ligand • T-shaped

1. (a) N. Selander, K. J. Szabó, *Chem. Rev.* **2011,** *111*, 2048-2076; (b) C. Gunanathan, D. Milstein, *Chem. Rev.* **2014,** *114*, 12024-12087; (c) J. Choi, A. H. R. MacArthur, M. Brookhart, A. S. Goldman, *Chem. Rev.* **2011,** *111*, 1761-1779; (d) R. Tanaka, M. Yamashita, K. Nozaki, *J. Am. Chem. Soc.* **2009,** *13*, 14168-14169; (e) E. Peris, R. H. Crabtree, *Chem. Soc. Rev.* **2018,** *47*, 1959-1968.
2. (a) S. Trofimenko, *Chem. Rev.* **1993,** *93*, 943-980; (b) J. G. Verkade, *Acc. Chem. Res.* **1993,** *26*, 483-489; (c) A. J. Gamble, J. M. Lynam, R. J. Thatcher, P. H. Walton, A. C. Whitwood, *Inorg. Chem.* **2013,** *52*, 4517-4527.
3. T. Suzuki, K. Fujimoto, Y. Takemoto, Y. Wasada-Tsutsui, T. Ozawa, T. Inomata, M. D. Fryzuk, H. Masuda, *ACS Catal.* **2018,** *8*, 3011-3015.
4. (a) K. Shiina, *J. Am. Chem. Soc.* **1972,** *94*, 9266-9267; (b) K. Komori, H. Oshita, Y. Mizobe, M. Hidai, M., *J. Am. Chem. Soc.* **1989,** *111*, 1939-1940; (c) M. Mori, *J. Organomet. Chem.* **2004,** *689*, 4210-4227; (d) H. Tanaka, A. Sasada, T. Kouno, M. Yuki, Y. Miyake, H. Nakanishi, Y. Nishibayashi, Y. Yoshizawa, *J. Am. Chem. Soc.* **2011,** *133*, 3498-3506; (e) R. Imayoshi, H. Tanaka, Y. Matsuo, M. Yuki, K. Nakajima, Y. Yoshizawa, Y. Nishibayashi, *Chem. Eur. J.* **2015,** *21*, 8905-8909; (f) M Yuki, Y. Miyake, Y. Nishibayashi, I. Wakiji, M. Hidai, *Organometallics* **2008,** *27*, 3947-3953; (g) R. B. Siedschlag, V. Bernales, K. D. Vogiatzis, N. Planas, L. J. Clouston, E. Bill, L. Gagliardi, C. C. Lu, *J. Am. Chem. Soc.* **2015,** *13*, 4638-4641; (h) R. C. Cammarota, L. J. Clouston, C. C. Lu, *Coord. Chem. Rev.* **2017,** *334*, 100-111; (i) D. E. Prokopchuk, E. S. Wiedner, E. D. Walter, C. V. Popescu, N. A. Piro, W. S. Kassel, R. M. Bullock, M. T. Mock, *J. Am. Chem. Soc.* **2017,** *139*, 9291-9301; (j) R. Araake, K. Sakadani, M. Tada, Y. Sakai, Y. Ohki, *J. Am. Chem. Soc.* **2017,** *139*, 5596-5606; (k) G. Ung, J. C. Peters, *Angew. Chem. Int. Ed.* **2015,** *54*, 532-535; (l) M. Yuki, H. Tanaka, K. Sasaki, Y. Miyake, K. Yoshizawa, Y. Nishibayashi, *Nat. Comm.* **2012,** *3*, 1254; (m) R. Imayoshi, K. Nakajima, Y. Nishibayashi, *Chem. Lett.* **2017,** *46*, 466-468; (n) A. J. Kendall, S. I. Johnson, R. M. Bullock, M. T. Mock, *J. Am. Chem. Soc.* **2018,** *140*, 2528-2536; (o) Y. Gao, G. Li, L. Deng, *J. Am. Chem. Soc.* **2018,** *140*, 2239-2250; (p) R. Imayoshi, K. Nakajima, J. Takaya, N. Iwasawa, Y. Nishibayashi, *Eur. J. Inorg. Chem.* **2017,** *2017*, 3769-3778.
5. Y. Tanabe, Y. Nishibayashi, *Coord. Chem. Rev.* **2019,** *389*, 73-93.
6. (a) L. Bourget-Merle, M. F. Lappert, J. R. Severn, *Chem. Rev.* **2002,** *102*, 3031-3066; (b) D. J. Mindiola, *Angew. Chem. Int. Ed.* **2009,** *48*, 6198-6200.
7. N. Lin, J. Yan, Z. Huang, C. Altier, M. Li, N. Carraco, M. Suyemoto, L. Johnston, S. Wang, Q. Wang, H. Fang, J. Caton-Williams, B. Wang, *Nucl. Acids Res.* **2007,** *35*, 5274-5274.
8. S. M. Crawford, C. A. Wheaton, V. Mishra, M. Stradiotto, *Can. J. Chem*. **2018,** *96*, 578-586.
9. A. Panda, M. Stender, R. J. Wright, M. M. Olmstead, P. Klavins, P. P. Power, *Inorg. Chem.* **2002,** *41*, 3909-3916.
10. (a) N. Okabe, Y. Muranishi, *Acta Cryst. C,* **2003,** *59*, m228-m230; (b) S. S. Anjana, B. Varghese, E. Prasad, E., *Acta Cryst. C,* **2017,** *73*, 492-497.
11. (a) S. S. Rozenel, R. Padilla, J. Arnold, *Inorg. Chem.* **2013,** *52*, 11544-11550; (b) R. P. Yu, J. M. Darmon, C. Milsmann, G. W. Margulieux, S. C. E. Stieber, S. DeBeer, P. J. Chirik, *J. Am. Chem. Soc.* **2013,** *135*, 13168-13184; (c) A. D. Ibrahim, K. Tokmic, M. R. Brennan, D. Kim, E. M. Matson, M. J. Nilges, J. A. Bertke, A. R. Fout, *Dalton Trans.* **2016,** *45*, 9805-9811; (d) T.-P. Lin, J. C. Peters, *J. Am. Chem. Soc.* **2013,** *135*, 15310-15313.
12. (a) M. Ingleson, H. Fan, M. Pink, J. Tomaszewski, K. G. Caulton, *J. Am. Chem. Soc.* **2006,** *128*, 1804-1805; (b) M. Ingleson, M. Pink, H. Fan, K. G. Caulton, *Inorg. Chem.* **2007,** *46*, 10321-10334; (c) L. S. Merz, C. K. Blasius, H. Wadepohl, L. H. Gade, *Inorg. Chem.* **2019,** *58*, 6102-6113.
13. D. F. Evans, *J. Chem. Sci.* **1959**, 2003-2005.
14. K. Zhu, P. D. Achord, X. Zhang, K. Krogh-Jespersen, A. S. Goldman, *J. Am. Chem. Soc.* **2004,** *126*, 13044-13053.
15. P. Liu, M. Wesolek, A. A. Danopoulos, P. Braunstein, *Organometallics* **2013,** *32*, 6286-6297.
16. D. E. Bergbreiter, J. M. Killough, *J. Am. Chem. Soc.* **1978,** *100*, 2126-2134.

10.1002/ejic.201901129

Entry for the Table of Contents (Please choose one layout)

Layout 2:

FULL PAPER

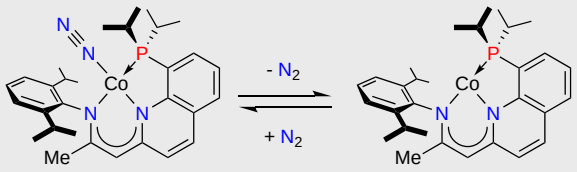

Co[QuiNacNacP]N_2 **Co[QuiNacNacP]**

Dinitrogen Cobalt Equilibrium*

*Corey A. Sanz, Carolin A. M. Stein, and Michael D. Fryzuk**

Page No. – Page No.

Synthesis of a T-Shaped Cobalt(I) Complex and its Dinitrogen Adduct

A new quinolone-based pincer ligand has been developed and its coordination chemistry with Co(II) examined. Upon reduction a square-planar dinitrogen cobalt(I) derivative is formed, which is in equilibrium with a T-shaped complex. A preliminary study shows that this system is capable of catalytically silylating dinitrogen.